UCLouvain

epl

École polytechnique de Louvain

Simulating the ocean circulation in the Arabian Gulf

Author: **Romain Voos**
Supervisor: **Emmanuel Hanert**
Readers: **Eric Deleersnijder, Jonathan Lambrechts**
Academic year 2022–2023
Master [120] in Mathematical Engineering

Abstract

The Arabian Gulf (hereafter, the Gulf) is a shallow semi-enclosed basin whose circulation is particularly complex. As it is the scene of daily oil exports around the world, the Gulf's circulation presents major climatic and economic challenges. It is primarily driven by water inflow from the Gulf of Oman and by density-driven and wind-driven flows within the Gulf. This study presents a high resolution model of the circulation in the Gulf, with a special focus on the the Gulf of Salwa, south of Bahrain, which we would like to investigate the connectivity with the rest of the Gulf. To achieve our aims, we will use the two-dimensional barotropic model as well as the Lagrangian particle tracker of the Second-generation Louvain-la-Neuve Ice-ocean Model (SLIM) on a unstructured mesh having a highest resolution of 500 m. The model has been validated with on-site observations off Qatar. The results allow to describe the hydrodynamics of the Gulf with important accuracy. We describe inter-seasonal and inter-annual changes in the Gulf's circulation. Then, we study the mean residence time of the Gulf of Salwa, which is the time for fictive particles to leave the region while being driven by the model currents. We state that the Gulf of Salwa is a pretty isolated area of within the Gulf.

Acknowledgments

I would like to start by thanking a number of people without whom this thesis would not have been possible.

First of all, I would like to thank my supervisor, Professor Emmanuel Hanert, for his incredible investment in this thesis project. He was there for me and my fellow students throughout the year to guide and support us in our work. His invaluable advice at the weekly meetings he organised on Fridays was of immense help to me.

Then, I would like to thank Lauranne, Riana, Colin and Thomas, the researchers who were always devoted to answering my questions and showing me the way forward when I was struggling. Their expertise in SLIM solved many issues and was crucial in my work.

I would also like to say a special thank you to my friends Amaury and Mathieu, with whom we worked so closely on this project. Our mutual aid was more than beneficial from every point of view.

Finally, I would like to thank my family for the enormous support, attention and motivation they gave me on a daily basis.

Contents

1 Introduction **3**
- 1.1 General context . . . 3
- 1.2 Previous ocean modelling studies of the Gulf . . . 5
- 1.3 Objectives . . . 9

2 Materials and methods **11**
- 2.1 The 2D model . . . 11
  - 2.1.1 The hydrodynamic model . . . 11
  - 2.1.2 The mesh . . . 14
  - 2.1.3 The model forcings . . . 15
- 2.2 The Lagrangian particle tracker . . . 16
  - 2.2.1 Particles position . . . 17
  - 2.2.2 Residence time . . . 18

3 Results **20**
- 3.1 Model validation . . . 20
- 3.2 General circulation . . . 23
- 3.3 Residence time study in the Gulf of Salwa . . . 28

4 Discussion **31**

5 Conclusion **33**

Chapter 1

Introduction

1.1 General context

Even though the first oil deposit of the Middle East was discovered by George Bernard Reynolds in Persia (Iran today) in 1908, the large scale oil production in the Arabian/Persian Gulf (hereafter, the Gulf) countries only began after World War II, in 1945 (*Oil Development in the Middle East* 2022). With the global industrial growth after the war, the oil demand massively increased since then and even more during the past 20 years (*Fossil Fuel Consumption* 2022). As a result, oil producing countries became wealthier and could afford better infrastructures to even further increase their production. The first countries to benefit from the oil boom in the Middle East were Kuwait, Iran, Iraq and Saudi Arabia.

Nowadays, Kuwait, Iran, Iraq, Saudi Arabia, Oman, United Arab Emirates and Qatar produce a lot of oil and gas, most of which is exported worldwide. These countries own 65% of the world's known oil reserves and produce over a third of the world's daily output (*Persian Gulf History,Arabian Gulf, Pars Sea ,* 2022). Saudi Arabia is the Gulf country with the largest oil reserves with 261 billion barrels. Then comes Iraq with 100 billion, then United Arab Emirates (98 billion), Kuwait (96.5 billion) and Iran (89 billion). The Gulf has also large gas reserves, with Iran and Qatar having respectively the world's second and third largest.

The development of hydrocarbons in the Gulf has certainly brought economic growth, but it also has a dark side. Indeed, oil and gas production sometimes brings important problems, the biggest of them being oil spills. The Gulf War oil spill (*Gulf War Oil Spill* 2023) was one of the largest oil spill in the Gulf's history. Namely, in 1991, Iraqi forces intentionally released between 4 and 6 million US barrels of oil, which represents between 480 000 m^3 and 720 000 m^3. The spill

flowed to the shores of Kuwait, Saudi Arabia, Bahrain, Iran, and Iraq. The risk of such spills is still present today, as 10 to 40 ships transporting oil pass through the Strait of Hormuz every day, on average (Batrawy 2019).

There are unfortunately several other examples of oil spills in the history of the Gulf. All of them are disasters for marine biodiversity, but also for human health. In fact, the Gulf's 1483 desalination plants are extremely important sources of its drinkable water and could absolutely not afford to be polluted by oil contaminated water. In 2000, Qatar supplied three quarters of its water demand with desalinated water (*Managing Water for Peace in the Middle East* 2023).

There are actually other environmental issues threatening the Gulf (Al Azhar et al. 2016). Harmful algae blooms (HABs) are also quite concerning. These are occurrences of excessive algal growth that can have detrimental effects on the marine ecosystem, human health, and economic activities in the Gulf. Al Shehhi, Gherboudj, and Ghedira 2014 overview the different HABs outbreaks recorded in the region, as well as their causes and impacts. It is claimed that the recent economic growth has led to important changes in marine ecosystem properties such as higher temperatures and salinity, higher evaporation rates or pollution. This thus put more stress on marine environment and generated more HABs outbreaks. These latter hurt marine life, water quality, human health and also desalination plants.

The common thread between these ecological disasters is that they both involve the water motion. Hence, they can be studied if we know the ocean circulation. The study of the ocean circulation of the Gulf consists in describing its hydrodynamics. This means to know how the water moves (its currents) in function of winds, tides, differences of temperature or density between water masses... It is totally possible to achieve this numerically, by creating an ocean model.

Ocean models are numerical models that describe the hydrodynamics of rivers, seas or oceans, which is the study of the water's motion. An accurate ocean model predicts the state of a particular marine region which includes several of its physical quantities such as temperature, salinity, pressure (from bottom to sea surface), water elevation level, current, etc. The main goal of this thesis will be to establish an accurate model of the hydrodynamics of the Gulf.

Such a model would allow to better address the oil spill problem. In fact, by knowing the currents of water, we can anticipate the spills trajectories and give a precise response to it. It is then possible to protect human activity zones and

marine ecosystems from potential contamination. Knowing risk areas also allows to locate new offshore infrastructures in the best possible way. Optimization of oil tankers or other types of ships routes is another contribution of hydrodynamic models.

In the same way, ocean models are able to help with other environmental issues. Having a good idea of the ocean physical processes in play permits to forecast the occurrences and transport dynamics of HABs. That way, efforts can be concentrated to stop or limit the spread. More generally, the knowledge of the ocean circulation is very useful to assess the impact of climate change on the Gulf. We can analyze the changes in its circulation under different scenarios of temperature and salinity increase or sea surface elevation rise. It is also helpful to organize efficient ocean cleanup operations.

1.2 Previous ocean modelling studies of the Gulf

In order to come up with a specific question of research that will be answered during this work, let us gather some useful information and results from other studies about the subject.

The Gulf is a semi-enclosed basin located in west Asia between the southern Iranian coasts and the northern Arabian peninsula. It is connected through the Strait of Hormuz to the Gulf of Oman, which is part of the Arabian Sea in the nort-hwest of the Indian Ocean. The Gulf is surrounded by Iran, Iraq, Kuwait, Bahrain, Qatar, Saudi Arabia, United Arab Emirates and Oman on the other side of the strait (see Figure 1.1). It has an average depth of 36 m, while its maximal depth of 120 m is reached near the Strait of Hormuz. On Figure 1.2, we see that the southern part is the more shallow one (less than 30 m depth) and the north part bordering Iran is more deep. The Gulf is about 1000 km long and 350 km wide at most. It and has a surface of 239 km^2 and a volume of 8780 km^3 (Pous, Lazure, and Carton 2015).

Figure 1.1: Geography around the Gulf (made with *QGIS* 2023)

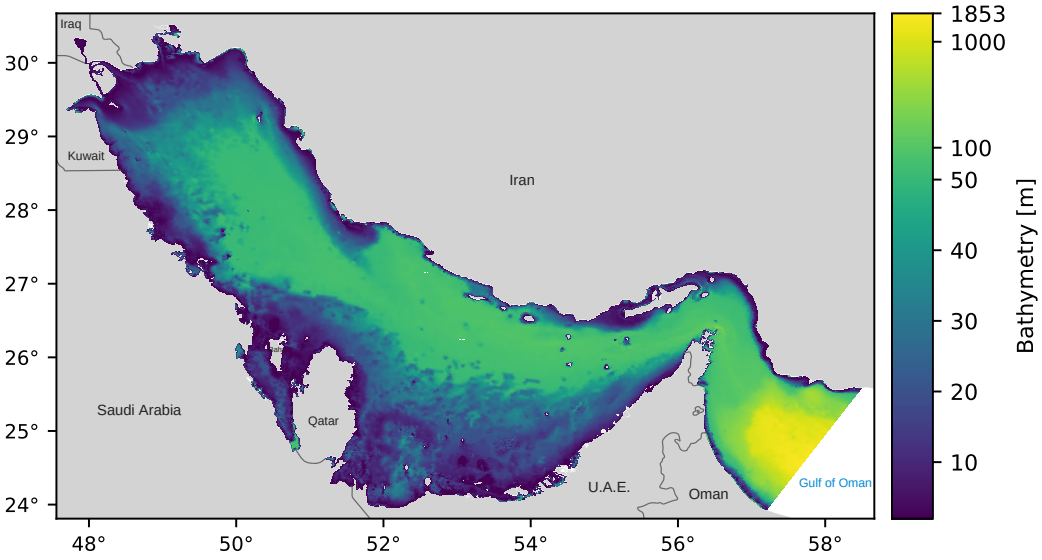

Figure 1.2: Bathymetry of the Gulf, with data from General Bathymetric Chart of the Oceans (Oceans 2023). The average depth is 36 m. The Southern Gulf is the most shallow part.

The predominant wind that blows above the Gulf is called Shamal and comes from the nort-hwest. It blows mostly during summer and winter. The high temperatures of the region create vertical gradients of temperature and, more importantly, of salinity. This will generate stratification between different water layers in the sea. It will also lead to many water exchanges through the Strait of Hormuz, but we will explain this in more details later.

Pous, Lazure, and Carton 2015 and Thoppil and Hogan 2010 showed that the general circulation in the Gulf is a barotropic cyclonic gyre from April to July. This means that the density of seawater is relatively uniform throughout the water column. In late summer, the gyre breaks down into some smaller eddies (see Figure 1.3). This does not change in winter because the wind intensifies and stratification decreases due to cooling. Dense salty water is then formed in winter in the north-west part of the Gulf and in the southern banks. There is a permanent southeastward deep current that makes dense water flow from the north-west towards the Strait of Hormuz all year long, while dense water formed in the southern banks only reach Hormuz from November to April. This is called density driven circulation. Thoppil and Hogan 2010 adds that the northwestward flowing Iranian Coastal Current from the Strait of Hormuz to north of Qatar forms the northern flank of the circulation and is the strongest current in the Gulf. The anticyclonic eddies formed during the winter reproduce every year but have a strong interannual variability.

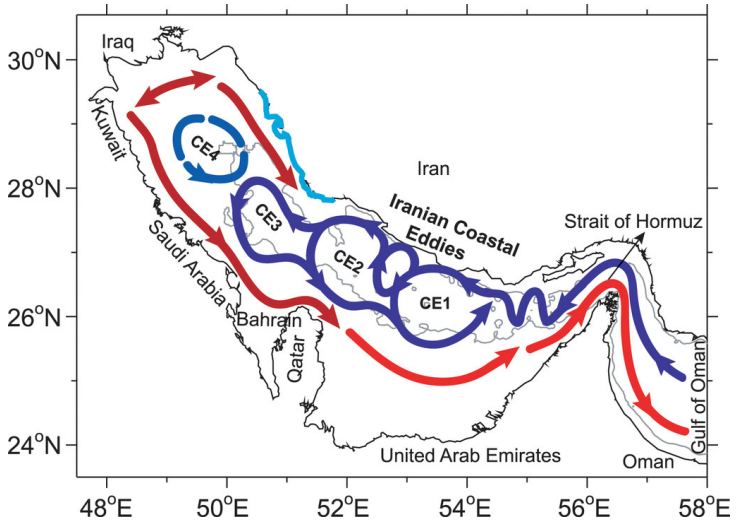

Figure 1.3: Circulation in the Persian Gulf. The general circulation becomes instable and breaks down into four Iranian Coastal Eddies, from Thoppil and Hogan 2010

According to Al Azhar et al. 2016, the inflow of less saline water from the Strait of Hormuz to the Gulf is stronger in summer than in winter (see Figure 1.4). This creates a high stratification in deep water areas. The densest waters are located in southern part of the Gulf which is more shallow. There is an outgoing flow to the Gulf of Oman of saline waters in the bottom layers with limited seasonal variability. The highest stratification are created because of the interaction between the inflow of low salinity in the northern coast and the outflow of high salinity in the southern coast near the Strait of Hormuz. These are also influenced by the strong vertical gradients of temperature (due to surface heating in summer and outflow of cold water in subsurface layer). The highest stratifications are observed in deep water areas located in the north-west part of the Gulf. Surface water from the Gulf of Oman is mixed with deeper water of the Gulf and this creates stratification.

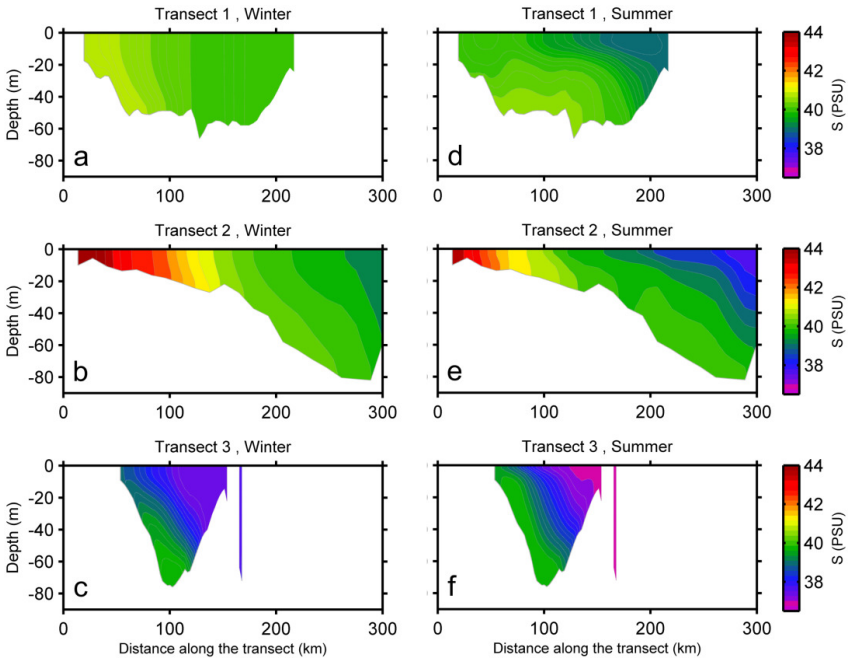

Figure 1.4: Seasonal averaged of salinity (psu) in winter (left: December–January–February) and summer (right: June–July–August) 1992 along (top) transect 1, (middle) transect 2, and (bottom) transect 3, from Al Azhar et al. 2016

These ocean modelling studies give a good general idea of the ocean circulation in the Gulf. However, they have certain limitations. The three dimensional model of Al Azhar et al. 2016 describes the inter-seasonal changes in the circulation, but

for the year 1992. The Gulf's circulation has reasonably changed since then as lots of coastal development and offshore infrastructures were constructed. The model of Hosseinibalam, Hassanzadeh, and Rezaei-Latifi 2011 was made from a structured grid, which mean that the low scaled interactions could not be captured. The study proposed by Hanert et al. 2023 with a two-dimensional multi scale mesh is accurate and describes the inter-seasonal changes of the circulation in the Gulf. It is claimed, though, that a three-dimensional model would be very appreciated in order to better represent the physical processes driving the ocean dynamics. Finally, the model of Pous, Lazure, and Carton 2015 is rather coarse, as the mesh reaches a maximal resolution of 3 km.

Other interesting results concern the Gulf of Salwa (hereafter GoS), south of Bahrain (see Figure 1.1). The model of Hanert et al. 2023 showed that some clockwise eddies were formed in the GoS. These are present all year long, but are stronger in winter and summer. Additionally, Joydas et al. 2015 states that the Gulf of Salwa is isolated from the rest of the Gulf and "Seasonal Cycles of Temperature, Salinity and Water Masses of the Western Arabian Gulf" n.d. also notes large differences of salinity and temperatures between the GoS and the Gulf. This coupled with the fact that the areas linking the GoS to the rest of the Gulf are very shallow makes it fair to wonder if the circulation in the GoS is truly connected with the one in the rest of the Gulf.

1.3 Objectives

In view of the previous studies modelling the ocean circulation of the Gulf, we can define the objectives of this thesis. The first and main objective is **to develop a multi scale two-dimensional model of the circulation of the whole Gulf**. The goal is to represent both the large scale density-driven circulation patterns as well as the small scale flow-topography interactions. To achieve this, the target accuracy of the mesh is of about 500 m, for the highest precision part. The model will be built based on recent forcing data, in order to take all infrastructures located along the coasts and offshore into account. We aim to describe the inter-seasonal and inter-annual variations of the Gulf's circulation patterns. Secondly, we will **focus the analysis on the Gulf of Salwa**, located south of Bahrain. We will try to determine if its circulation is connected with the rest of the Gulf or not.

To achieve this, we will use the Second-generation Louvain-la-Neuve Ice-ocean Model, called "SLIM" from now on (*SLIM – Second-generation Louvain-la-Neuve Ice-ocean Model* 2022). SLIM is a multi scale ocean model. More precisely, we will use the 2D version of SLIM as well as its Lagrangian particle tracker. The model

will be validated with current velocity data measured in Doha Bay and offshore of Ras Laffan.

On the other hand, it would be very appropriate to also build a three-dimensional model of the Gulf's circulation. As stated above, it would help to understand the physical processes in play with an even greater precision. Indeed, we know that stratification is an important factor in the formation of the main currents. This can only be captured by a 3D model, as it computes temperatures and salinity at different depths of the water, unlike a 2D one. Initially, this challenge was also part of this work. Unfortunately, for practical and technical reasons, it has not been possible to get SLIM-3D to work properly within the allotted time.

Here is an outline of this work. First, we will present the model in details and all the necessary parameters and involved data to make it work correctly. Then, we will be able to present the results of the main circulation patterns of the Gulf and compare them to the available observations. After that, we will focus on the inter-seasonal and inter-annual variations of the circulation. Next, we will investigate the connectivity between the Gulf of Salwa and the rest of the Gulf. Finally, we will discuss the results and put them into perspective with the literature.

Chapter 2

Materials and methods

The goal of this work is to simulate the ocean circulation in the Gulf. To achieve this, we will use SLIM, a sophisticated hydrodynamic model that has already proven itself many times. SLIM is a hydrodynamic model that uses an unstructured mesh to simulate flows at different scales. Based on the Discontinuous Galerkin finite element method, it computes water flows going from rivers to coastal oceans with high accuracy. We will explain the broad outlines of the method later.

SLIM has got many features which makes it a very flexible tool usable in many areas of applications. The main parts of the model are SLIM1D (for river flows), SLIM2D (for shallow barotropic flows), SLIM3D (for complex flows where the vertical aspects of the circulation cannot be neglected), a Lagrangian particle tracker (for the transport of larvae or debris) and a transport model (for the dynamics of tracers such as pollutants and sediments). In this work, we will be using SLIM2D and the Lagrangian particle tracker.

2.1 The 2D model

2.1.1 The hydrodynamic model

The two-dimensional version of SLIM can be applied if the effects of the depth of the water can be neglected. It is the case in shallow water because the wind and tides will be sufficient to keep the water column well mixed. We say then that the flows are barotropic. This assumption can reasonably be applied in our study region as the Gulf is a rather shallow basin (average depth of 36 m, see figure 1.2). However, it is good to keep in mind that we are giving up some degree of precision that would be present in the three-dimensional model. In fact, SLIM3D solves the physical equations through the entire depth of the water. It is thus able to

highlight variations of temperature and salinity along the vertical axis. In the case of this study, these are especially important in summer, when evaporation leads to important stratification. This being said, the 2D model is also entirely appropriate here.

The model describes the depth-averaged shallow water equations for the surface elevation and the horizontal velocity. The equations read as (Dobbelaere 2018, Verbiest 2022, Hanert et al. 2023, Soupart 2018) :

$$\frac{\partial \eta}{\partial t} + \nabla \cdot (H\mathbf{u}) = 0 \tag{2.1}$$

$$\frac{\partial \mathbf{u}}{\partial t} + \mathbf{u} \cdot \nabla \mathbf{u} = -f\mathbf{e}_z \times \mathbf{u} - g\nabla\eta - \frac{g||\mathbf{u}||\mathbf{u}}{C^2 H} + \frac{\boldsymbol{\tau}}{\rho H} + \frac{1}{H}\nabla \cdot [H\nu(\nabla \mathbf{u})] + F_{gc} \tag{2.2}$$

The first equation is the depth-integrated continuity equation. It states the conservation of mass : the net water flow into or out of a given region must be balanced by the change in sea surface elevation. The second one is the momentum equation. It represents the conservation of momentum in the horizontal direction. In other words, it describes all the factors that influence the behavior of the horizontal velocity. All involved physical quantities are reported hereunder.

Variables :

- η $[m]$: is the sea surface elevation above a certain reference depth level (see figure 2.1).
- $\mathbf{u} = (u, v)$ $[\frac{m}{s}]$ is the depth-averaged horizontal velocity vector. u is the x component (going eastwards) of the velocity while v is its component in the y direction (going northwards).

There are thus 3 variables as the last equation is actually written in vector form. η is only derived with respect to time and the two last variables are derived with respect to x, y and t which are the coordinates of the 2D horizontal plane and the time, respectively.

Parameters and constants :

- H $[m]$ is the total water column depth such that $H = h + \eta$, where h is the bathymetry (see figure 2.1).
- f $[\frac{1}{s}]$ is the Coriolis factor. It is computed as followed : $f = 2\Omega \sin(\theta)$, where $\Omega = 7.29$ $[\frac{rad}{s}]$ is the angular rotation speed of the Earth and θ is the latitude.
- $\mathbf{e}_z$ is the upwards pointing unit vector.

- g $[\frac{m}{s^2}]$ is the acceleration due to gravity ($g = 9.81 \frac{m}{s^2}$).
- C $[\frac{m^{1/2}}{s}]$ is the Chezy bottom-stress coefficient. This coefficient is defined as $C = \frac{H^{1/6}}{n}$, where n is the Manning coefficient. Here, we take $n = 0.022$ $\frac{s}{m^{1/3}}$.
- $\boldsymbol{\tau}$ $[\frac{kg}{ms^2}]$ is the surface wind stress. It is given by the following formula : $\boldsymbol{\tau} = \rho_{air} C_D ||\mathbf{u}_{10}|| \mathbf{u}_{10}$. Here, ρ_{air} is the air density ($\rho_{air} \approx 1.204 \frac{kg}{m^3}$), $\mathbf{u}_{10}$ is the wind velocity 10 meters above the see surface and C_D is the drag coefficient. C_D is computed with the Smith and Banke formula (Smith and Banke 1975) : $C_D = 10^{-3}(\alpha + \beta ||\mathbf{u}_{10}||)$, where $\alpha = 0.63$ and $\beta = 6.61^{-2} \frac{s}{m}$.
- ρ $[\frac{kg}{m^3}]$ is the water density ($\rho = 1027$ $\frac{kg}{m^3}$).
- ν $[\frac{m^2}{s}]$ is the horizontal kinematic viscosity of water. It is computed using Smagorinsky parametrization (Smagorinsky 1963) :
$\nu = (\tilde{C_S}\Delta)^2 \sqrt{2(\frac{\partial u}{\partial x})^2 + 2(\frac{\partial v}{\partial y})^2 + (\frac{\partial u}{\partial x} + \frac{\partial v}{\partial y})^2}$, with the Smagorinsky coefficient $\tilde{C_S} = 0.1$ and Δ the size of the local element of the mesh.
- The last term F_{gc} is the global circulation forcing term. Its goal is to keep the velocity computed by SLIM $\mathbf{u}$ close to a real measured velocity $\mathbf{u}_*$ (section 2.1.3), where the 2D model is not able to approximate the flows. $F_{gc} = \gamma(\mathbf{u}_* - \mathbf{u})$, with γ $[\frac{1}{s}]$ being 0 at all depths below 50 m. Otherwise, its value increases linearly from $5 \cdot 10^{-6}$ $\frac{1}{s}$ at 50 m to $3 \cdot 10^{-5}$ $\frac{1}{s}$ at 300 m of depth and beyond.

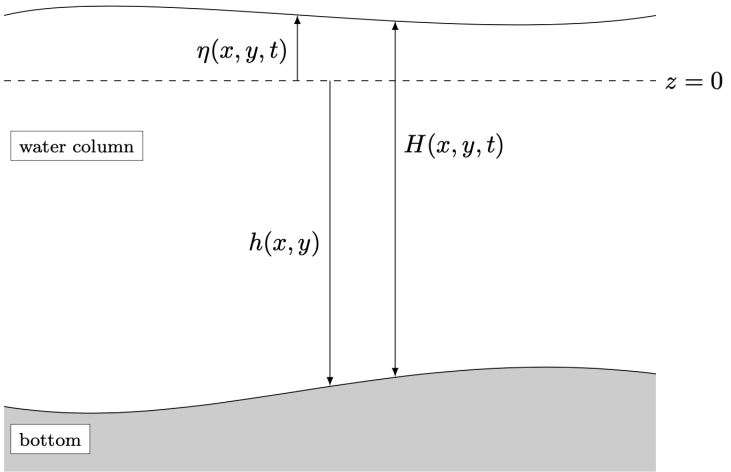

Figure 2.1: Schematic representation of the total water column height $H = \eta + h$, from Gourgue n.d. η is computed by the model and the bathymetry h is a model forcing (see section 2.1.3)

To solve these equations numerically, SLIM uses the Discontinuous Galerkin finite element method. Briefly speaking, the finite element method is a numerical method that allows to approximate the solution of partial derivative equations arising from many engineering fields such as electrodynamics, fluid mechanics or heat transfer. The method works as follows. We first create a mesh by dividing the domain where the equations apply into smaller parts, called "finite elements". Each node of the mesh represents one unknown point where we will compute the numerical solution. The equations of the underlying physics are applied on each element. Then, the equations from all elements are assembled and the whole system is solved using the boundary conditions of the original problem (*Discontinuous Galerkin Method* 2023).

2.1.2 The mesh

The first step in the process of performing a simulation of the ocean flows using SLIM is to create a mesh. To do this, we begin by generating a shapefile with the software QGIS (*QGIS* 2023) that will set up the domain boundaries and its topography. The topography of the coastlines is downloaded on OpenStreetMap (*Coastlines* 2023). There can be closed boundaries (for example coasts) or open ones (if we cut the domain through the ocean). Then, we make a mesh from it using GMSH (Geuzaine and Remacle 2009). The resolution of the mesh can be adapted to be very high near the coasts or other interest regions and at the same time rather coarse far from the boundaries. In this way, the important places are accurately described, but the computing time is kept reasonable. This kind of mesh where the resolution is not homogeneous is called an unstructured mesh. The mesh has to be sufficiently highly resolved (its elements have to be locally sufficiently small) so that the currents are modeled with accuracy. In addition to that, the more the mesh is highly resolved, the more we can model small islands or artificial structures in the ocean that will also influence the general circulation.

The elements of the mesh have a minimum size s_0 if they are located within a distance d_0 from the coasts, a maximum size s_1 if they are beyond a distance d_1 from any coast and a size that evolves linearly between the two if they are located in the interval $[d_0, d_1]$. In other words,

$$\Delta(d) = \begin{cases} s_0 & \text{if } d \leq d_0 \\ s_0 \frac{(d_1 - d)}{(d_1 - d_0)} + s_1 \frac{(d - d_0)}{(d_1 - d_0)} & \text{if } d_0 < d < d_1 \\ s_1 & \text{if } d_1 \leq d \end{cases}$$

Here, the values of those parameters were chosen the following way : $d_0 = 2.5$ km, $d_1 = 10$ km, $s_0 = 500$ m and $s_1 = 5$ km. This ensures that 10 km wide layer

along the coasts is sufficiently well resolved. The mesh I used for the simulations is represented on figure 2.2. It counts 322 531 triangles and 170 439 nodes.

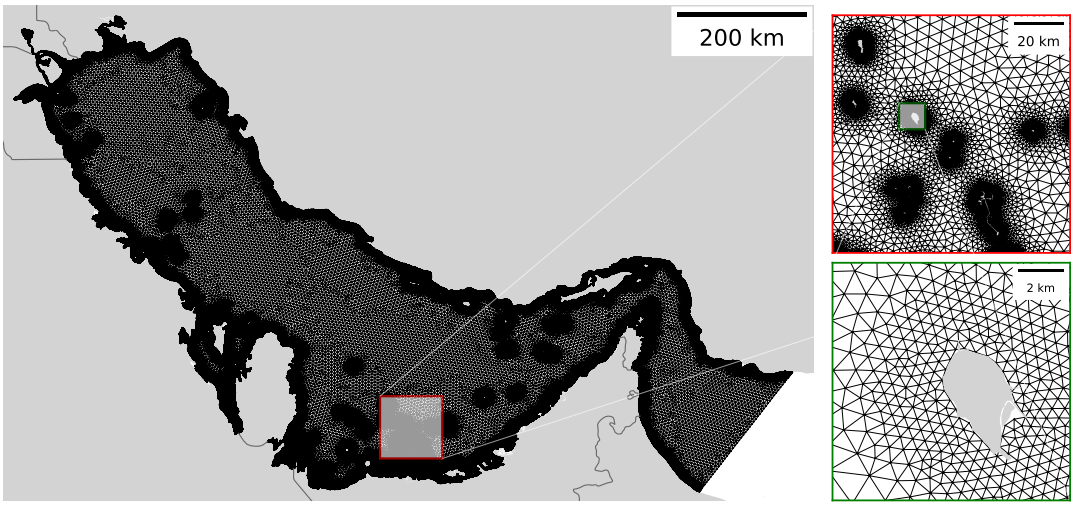

Figure 2.2: Unstructured 2D mesh of the Gulf with one open boundary in the south-east of the Gulf. The element sizes range from 500 m to 5 km

2.1.3 The model forcings

Now that we have a mesh, we need to download the model forcings. This includes all the external data that will be given to the model in order to perform the simulations. The forcings depend of course on the time of the simulation and on its geographical location.

The bathymetry, which is the depth of the sea floor, is given by the open source GEBCO (General Bathymetric Chart of the Oceans Oceans 2023). It is used to determine the value of h throughout the domain (see figures 1.2 and 2.1). Then, the wind velocity and atmospheric pressure data are downloaded from ERA5 (Hersbach et al. 2020) with the Copernicus Climate Data Store API (2023) in order the get the value of $\mathbf{u}_{10}$. Finally, to find the data resulting in the $\mathbf{u}_*$ parameter, the tidal velocities are forced with the TPXO9-atlas dataset (*OSU TPXO Tide Models - TPXO9-atlas* 2023) and the large-scale current velocities are downloaded from the Copernicus Marine Service (*Copernicus Marine Data Store* 2023).

Note that the bathymetry used in the model is not exactly the same as the one extracted from GEBCO. Indeed, we need to treat it in order to avoid numerical instabilities and crashes. We first define a parameter called `min_depth` which sets

the minimal depth value that can be taken by $h(x, y)$. Here, it is set to 2 m. That way, the domain is insured to be under water at anytime, and the approximation is not too coarse at the same time. Then, we operate a smoothing of the bathymetry. For each element of the mesh, the difference between the bathymetry at each node and the mean bathymetry of the element will be reduced by a certain factor. The goal is to impose a maximum variation of bathymetry on all elements. Here is a pseudo-code of the simplified smoothing algorithm :

Algorithm 1 smoothing_bathymetry(mesh, bathy, $c = 0.5$)

```
for triangle in mesh do
    b_1, b_2, b_3 = bathy[node_1], bathy[node_2], bathy[node_3]
    b_max = max(b_1, b_2, b_3)
    b_min = min(b_1, b_2, b_3)
    b_av = (b_1 + b_2 + b_3)/3
    δ = b_max − b_min
    d = c · b_max
    f = min(d/δ, 1)
    for node in triangle do
        b_i = b_av + f(b_i − b_av)
        bathy[node_i] = b_i
    end for
end for
return bathy
```

In a nutshell, the bathymetry at each node will be brought closer to the mean bathymetry of the triangle, according to the coefficient c, which value is 0.5. By reducing c, we would increase the smoothing. We see that if $d > \delta$, the bathymetry is not smoothed at all. Also, the bigger is δ, the more the bathymetry is smoothed. Several iterations of this algorithm will be applied until the bathymety is sufficiently smoothed (until $1 - f < 0.01$).

The downloading of the forcings and its treatment is done in a premilinary step called "preprocessing". Then, the run itself is executed and the equations are solved through the temporal iterations.

2.2 The Lagrangian particle tracker

The other powerful SLIM tool that we will use during this thesis is its Lagrangian particle tracker. A Lagrangian particle tracker (or LPT) is a numerical tool that simulates the motion of Lagrangian particles within a flow. Lagrangian particles

are small fictive elements that move through the flow field, allowing the tracking of their positions and properties over time. By integrating the hydrodynamics computed by SLIM2D, the LPT model of SLIM can be used to represent many different types of particles. For example, we could study the transport of plastic debris, the connectivity between coral reefs or the dispersal of turtle juveniles.

2.2.1 Particles position

The LPT uses a random walk formulation of the 2D advection-diffusion equations (Spagnol et al. 2002, Hunter, Craig, and Phillips 1993) . The discretized scheme reads as follows :

$$\mathbf{x}_{n+1} = \mathbf{x}_n + \mathbf{v}_n \Delta t + \frac{\mathbf{R}_n}{\sqrt{r}} \sqrt{2K\Delta t}, \tag{2.3}$$

with

$$\mathbf{v}_n = \left(\mathbf{u} + \frac{K}{H} \nabla H + \nabla K \right) \Big|_{\mathbf{x}_n}. \tag{2.4}$$

Here, $\mathbf{x}_n$ and $\mathbf{x}_{n+1}$ are the vectors of the particles positions at time iterations n and $n+1$, respectively. The model time step Δt is set to 450 s. K is the horizontal diffusivity coefficient. $\mathbf{u} = \mathbf{u}(\mathbf{x}, t)$ is the instantaneous depth-averaged horizontal water velocity modeled by SLIM2D. H is the water column depth, as defined in figure 2.1. $\mathbf{R}_n$ is a random two-dimensional vector of numbers. It has a zero mean and a variance r (the vector $\frac{\mathbf{R}_n}{\sqrt{r}}$ is then a random vector of zero mean and unit variance).

Equation 2.3 can be split in two parts. The first term $\mathbf{v}_n \Delta t$ we add to $d\mathbf{x} = \mathbf{x}_{n+1} - \mathbf{x}_n$ is the deterministic part of the equation. It takes the water elevation H and depth-averaged velocity $\mathbf{u}$ as input to state that the particles will move according to the currents computed by SLIM. Remark that the velocity is corrected with $\frac{K}{H}\nabla H + \nabla K$ to increase the displacement of particles in regions where diffusivity is high and in shallow regions. The horizontal diffusivity is defined with the Okubo formulation (Okubo 1971) :

$$K = \alpha \Delta^{1.15} [\frac{m^2}{s}], \tag{2.5}$$

where α is set to 0.041 $\frac{m^{0.85}}{s}$ and Δ is the local element size.

The other term is the stochastic part, which creates the randomness of the movement. It models the random sub-grid scale turbulence effects and also the uncertainty of events that can happen in the transport of particles.

2.2.2 Residence time

Now, the important output of the LPT we will focus on here is not much the final positions of the particles, but rather the amount of time they need to leave the region of interest. We call it the residence time. We can define the residence time from different angles : there is the residence time of a single particle, the residence time of a mesh element and the mean residence time of the particles inside a region. Deleersnijder 2017 defines the latter for particles released in the domain at time $t = t_0$ as

$$\bar{\theta}(t_0) = \frac{1}{m(t_0)} \int_{t_0}^{\infty} m(t)dt, \tag{2.6}$$

where $m(t)$ is the number of particles inside the domain at time t. Here, we assume that $m(t)$ decreases over time and that $\lim_{t\to\infty} m(t) = 0$ (the number of remaining particles inside the domain will eventually be arbitrarily small). This is a continuous time definition, but as we will apply a numerical algorithm, we will need a discrete definition as well.

Here is how the LPT is executed. We first define a region of interest. In our case, the Gulf of Salwa. The region is delimited by closed boundaries (i.e. coasts) and open boundaries, which are piecewise straight lines going from one coast to another across the domain (see figure 3.7). Let us call this region D. We say that a particle leaves D if its position goes beyond an open boundary. The model virtually releases particles from all triangles whose centroid [1] is inside D. Let us denote that number N. There is one particle released in each of these triangles at their centroid every Δ_{seed} amount of time during a period T_{seed}. Here, $\Delta_{seed} = 12$ hours and $T_{seed} = 15$ days. There will thus be a total of $P = \frac{24}{12} \times 15 = 30$ particles released from every triangle whose centroid is inside D during the seeding period.

We will run the LPT algorithm going from $t = t_0$ to $t = t_n$. At each iteration, we release particles in the centriods of the triangles, if we are still in the seeding period (if $t \leq T_{seed}$). From the moment a particle is released in D, two pieces of information are recorded about it. The first one is the element from where it has been released (its starting position). The second one is the total time it has spent inside D, namely its residence time. It is initially set to 0 s. Let us denote by $\theta_{i,j}(t)$ the residence time of particle $j \in \{1, \ldots, P\}$ that started from triangle $i \in \{1, \ldots, N\}$ at time $t \in [t_0, t_n]$. Then, we increment the particles position by $d\mathbf{x}$ (see equation 2.3). There are then three possible scenarios for the updated position of a particle.

[1] The centroid of a triangle is the mean point of its vertices. For example, if the coordinates of a triangles vertices are given by $(x_1, y_1), (x_2, y_2)$ and (x_3, y_3), its centroid will be located at $(\frac{x_1+x_2+x_3}{3}, \frac{y_1+y_2+y_3}{3})$.

(a) The trajectory of the particle movement between the old and the new position has not crossed any closed or open boundary.

(b) The trajectory of the particle movement between the old and the new position has crossed a closed boundary. In that case, the component of the movement perpendicular to the edge of the triangle that forms the closed boundary is limited up to the boundary, while the parallel component to the edge is unchanged. The particle will thus slide along the boundary, but it will not rebound on it or settle on it.

(c) The trajectory of the particle movement between the old and the new position has crossed an open boundary. The particle is then outside D. In that case, its residence time is frozen, it will no longer increase.

Finally, we remove from the set of particles all the particles that just left D and increment the residence times of the others with Δt (see equation 2.3).

We can now define the residence time of element i at time t as

$$\theta_i(t) = \frac{1}{m_i(t)} \sum_{j=1}^{m_i(t)} \theta_{i,j}(t), \tag{2.7}$$

with $m_i(t)$ the number of particles released from element i since t_0 ($0 \leq m_i(t) \leq P, \forall t \in [t_0, t_n]$). The mean residence time of all particles released in D will be computed as the weighted average residence time of all elements in D at the final time of the simulation :

$$\bar{\theta} = \frac{\sum_{i=1}^{N} \theta_i(t_n) a_i}{\sum_{i=1}^{N} a_i}, \tag{2.8}$$

where a_i is the area of triangle i. Unlike Deleersnijder 2017, we released the particles progressively during a seeding period and not all at once at the beginning. Lastly, it is important to notice that the elements sizes are taken into account, which is not the case in a classic arithmetical mean of the elemental residence times. There are more elements near the coasts than in the center part of D, so their residence times would have more weight in a classic arithmetical mean residence time and it would thus have been biased.

Chapter 3

Results

3.1 Model validation

After explaining how the model is constructed and how it gets the forcing data as input, we can now perform real simulations. In this chapter, we will present our different results, but before that, let us test the model with actual on-site observations. This first step is indeed necessary in order to be sure that our model is working correctly enough and that the results are sufficiently accurate. The goal here is to evaluate if the numerical model is consistent with the measured reality.

The model was tested at two observation points in the Gulf : one located 2.5 km off Fuwairit, on the north-east coast of Qatar and the other in the Doha Bay, also in Qatar, at 2 km from the coastline (see Figure 3.1). At Fuwairit, we have both sea surface elevation and current velocity data that were measured every 10 minutes during October 29 - November 26, 2019. In Doha Bay, only sea surface elevation data are available every 10 minutes during December 8, 2021 - January 17, 2022. The measurements were made by means of a Seaguard Recording Current Meter (RCM) fitted with wave and tide sensors.

Figure 3.1: Location of the two validation points : Fuwairit is to the north-east and Doha Bay is on the east coast of Qatar (*Plans* 2023)

On figures 3.2, a comparison between the current directions and speeds of the model and the observations at Fuwairit is presented. Each arrow represents one current vector $\mathbf{u} = (u, v)$ evaluated at a specific time and the same location. There is one arrow per hour between October 29, 2019 and November 26, 2019. We see that the model fits quite well to the northwestwards and southeastwards observed currents. These cyclic alternations in directions are due to the tidal effects. The model also reproduces the event that occurred during 19 - 22 November, where Shamal blew strongly to prevent currents to flow in the north-west direction. On the circular graph, we see that the directions are well reproduced by the model, while the current speeds are sometimes overestimated or underestimated by the model. The root mean square error (RMSE) of the current speeds is of 4.5 cm/s and of 33.8° for the directions.

On Figure 3.3, we can see the validation of the sea surface elevation η, for both Fuwairit (2019) and Doha Bay (2021) observation sites. Again, the tidal effects are clearly well reproduced by the model, which is quite encouraging for the rest of this work. The root mean square errors (RMSE) are of 8.2 cm for Fuwairit and 10.5 cm for Doha Bay.

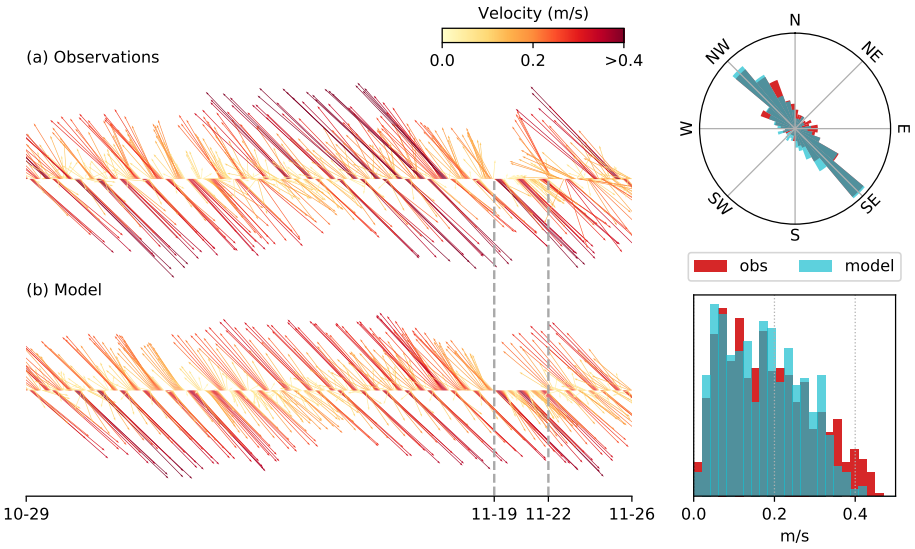

Figure 3.2: Comparison between the observed and modelled currents off Fuwairit, during 29 Oct - 26 Nov, 2019 and histograms of the current direction and amplitude. The model correctly reproduces both the current speed and direction.

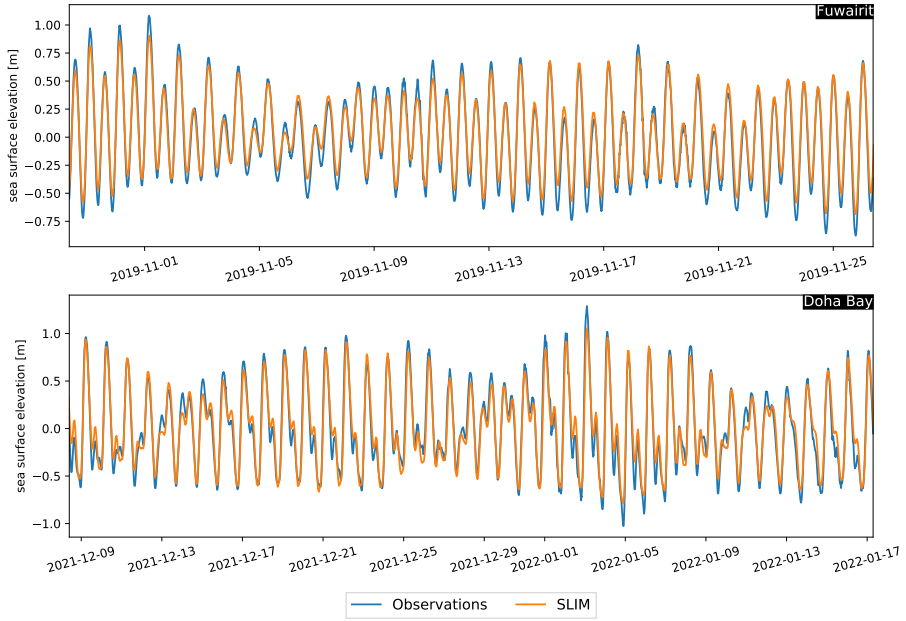

Figure 3.3: Comparison between the observed and modelled sea surface elevation η off Fuwairit (29 Oct - 26 Nov, 2019) and in Doha Bay (08 Dec 2021 - 17 Jan 2022). In both cases, the model correctly reproduces the tidal cycles.

3.2 General circulation

After validating the model, we can now start to use it to accomplish the main goal of this work : assessing the general circulation in the Gulf. On figures 3.4, we represent the monthly averaged current speeds and streamlines of the circulation in the entire Gulf, during winter (January), spring (April), summer (July) and autumn (October) 2019. The same is shown for years 2020 and 2022 on figures 3.5 and 3.6, respectively.

On each plot, the streamlines correspond to the directions of the vector field $\mathbf{u} = (u, v)$, while the color map covers the values of the magnitude of $\mathbf{u}$, which is $\sqrt{u^2 + v^2}$. The scale values range between 0 m/s and 0.586 m/s, which is the minimum value of $\mathbf{u}^*$ over all 12 plots ($\mathbf{u}^*$ is the maximum value of the current speed). The scale values increase linearly until 0.03 m/s, and then the scale becomes logarithmic until 0.586 m/s. Additionally, the maximal velocity $\mathbf{u}^*$ of each map is indicated in their upper right corner.

If we look at figure 3.5 that shows year 2020, we can break down the model's circulation throughout the seasons of the year as follows. In July, a big counterclockwise gyre dominates the circulation. It is located in the northern Gulf, just below the Iranian coasts. We see that it starts to split into two small, but intense eddies. In October, the gyre has definitely split into 4 smaller and slower eddies. The velocities inside the Gulf have decreased everywhere. The eddies are present in the north-west, but the one in the center is the strongest. In January, a large-scale circulation pattern appears again, with a low intensity little gyre forming to the north-west. On the other hand, the other gyre is much stronger and carries in its wake the water from eastern Qatar to the Strait of Hormuz, across almost the entire width of the Gulf. In April, the currents have slowed down and the north-west and southern parts become a bit messy. A big gyre located along Iranian coast is starting to form, before arriving at its peak in July.

The yearly scheme in the circulation patterns is not totally constant, but sees some inter-annual variations. Compared to 2020, the current intensities were higher throughout 2019, except in April. In July, the gyre was larger than in 2020, impacting almost the whole Gulf, not just its northern part. This important gyre was already there in the central part in April, even if it was then less strong. In 2022, the gyre of July is clearly broken down into two big counterclockwise eddies instead of one gyre. In October, the multiple eddies are more intense than in 2020.

Regarding water exchanges through the Strait of Hormuz, the most important exchanges occur every year in summer. These are fresh water masses coming from the Gulf of Oman. The currents through the strait are also important in October

2019 and in January 2020. In 2022, currents flowing through the strait are not so much in a straight line, but rather form gentle eddies within the strait. This means that the density driven circulation modelled by SLIM also has inter-annual variations.

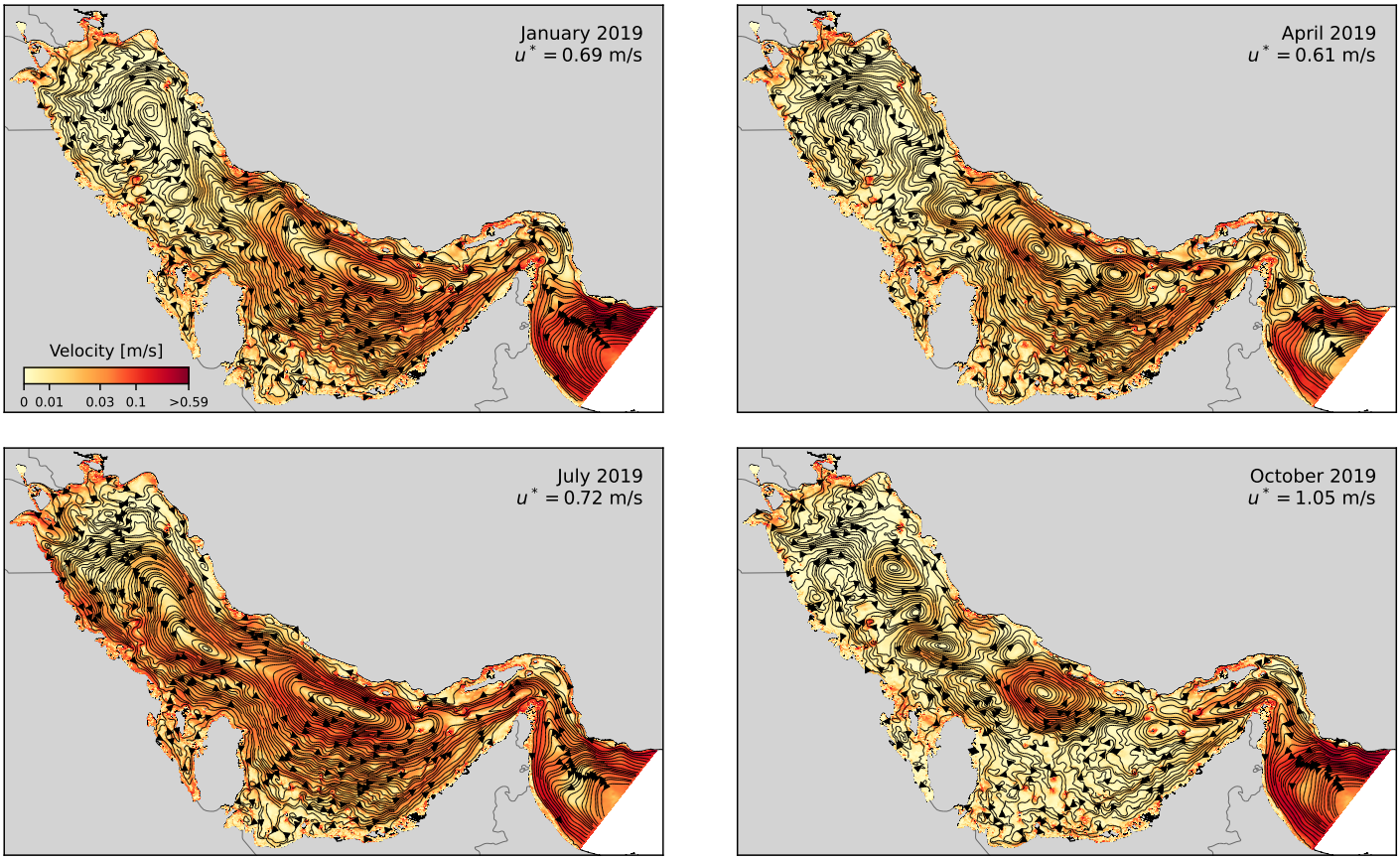

Figure 3.4: General monthly averaged circulation in the Gulf during January, April, July and October 2019. The color scale is the same for the four figures and indicates the current speeds computed by the model. $\mathbf{u}^*$ is the maximal speed value. The circulation is a counterclockwise gyre in July that splits into smaller eddies in autumn. Then some mid-scale eddies appear in January and April. Water exchanges with the Gulf of Oman are very important during summer.

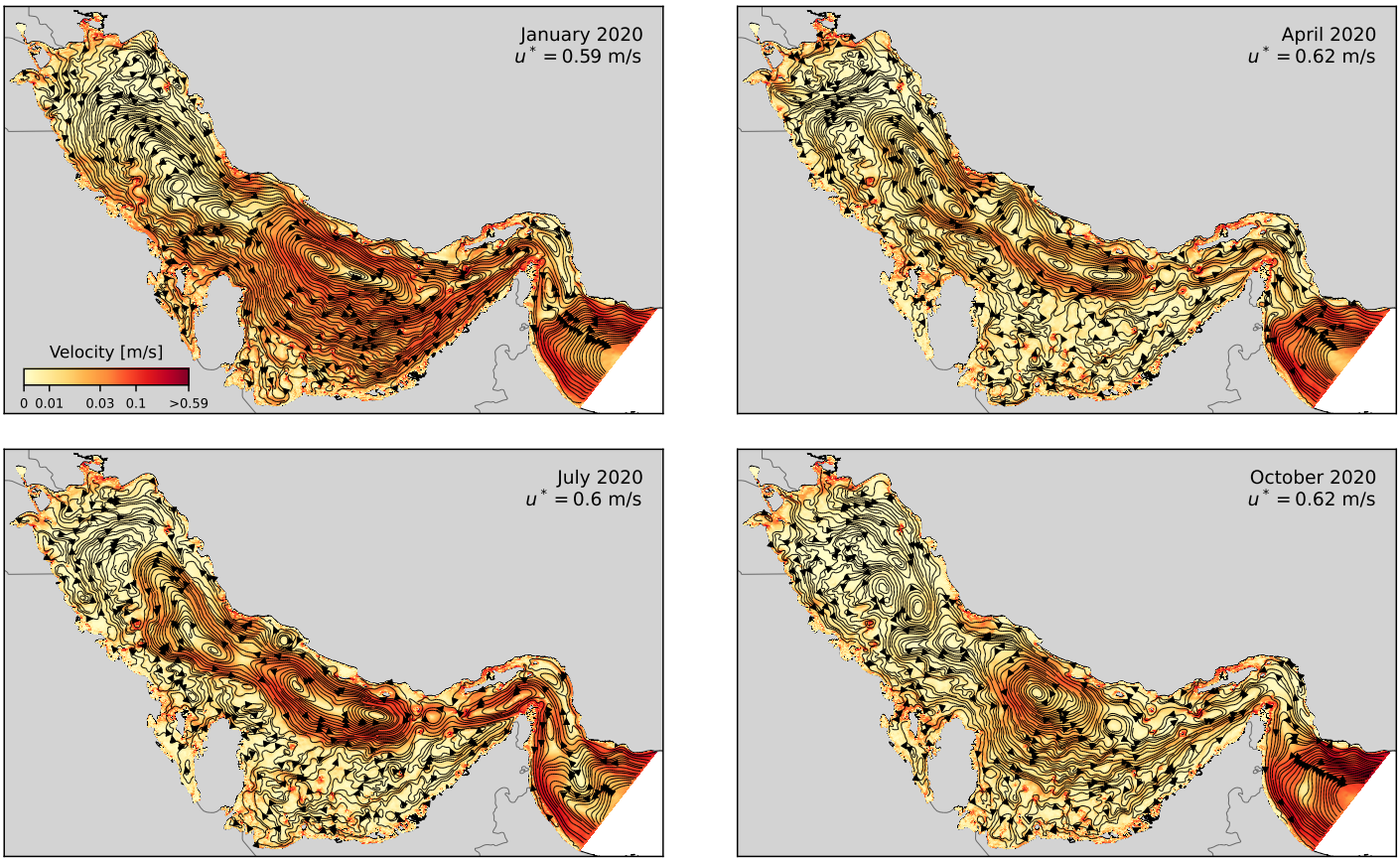

Figure 3.5: General monthly averaged circulation in the Gulf during January, April, July and October 2020 The color scale is the same for the four figures and indicates the current speeds computed by the model. $\mathbf{u}^*$ is the maximal speed value. The circulation is a counterclockwise gyre in July that splits into smaller eddies in autumn. Then, some mid-scale eddies appear in January and April.

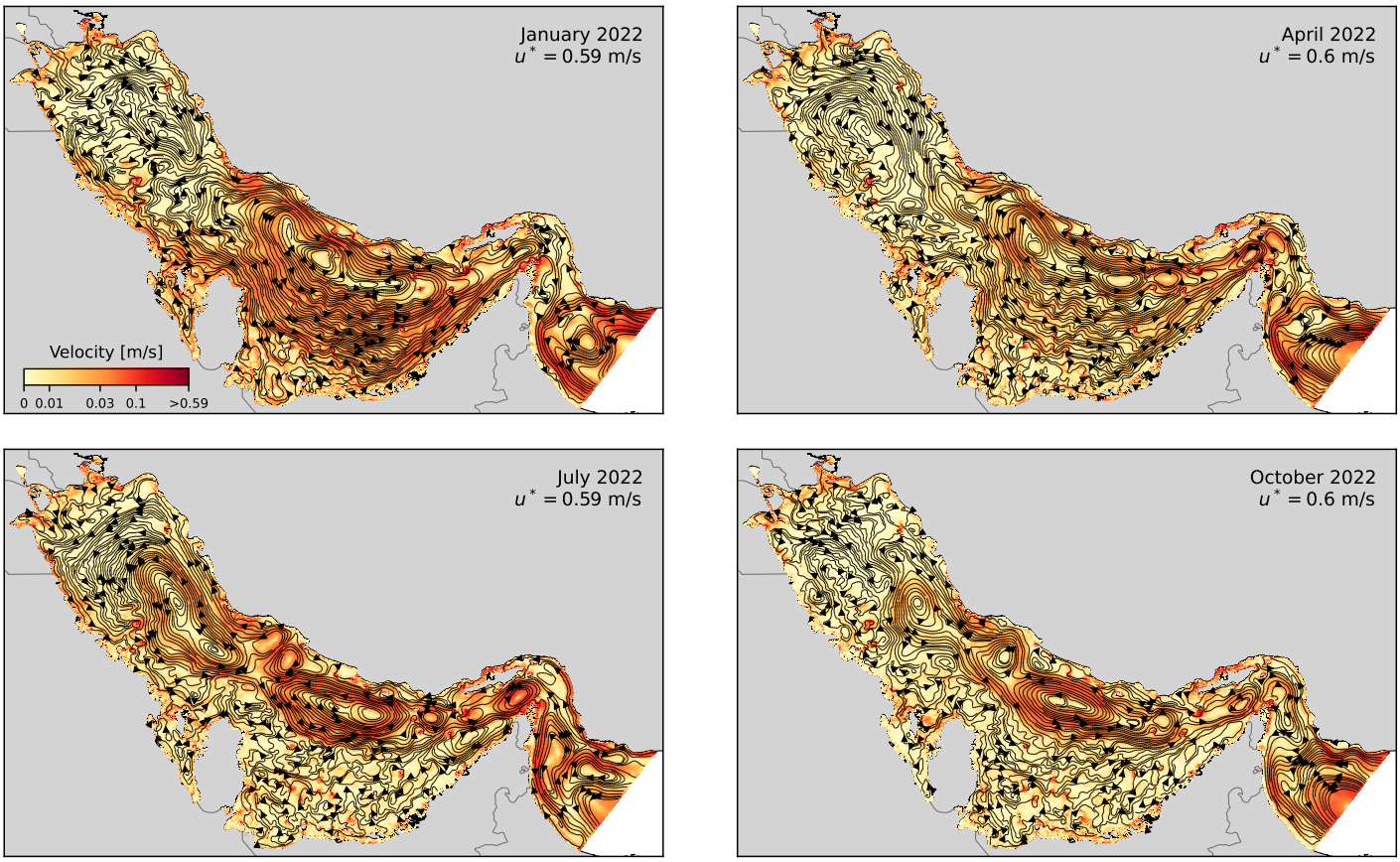

Figure 3.6: General monthly averaged circulation in the Gulf during January, April, July and October 2022. The color scale is the same for the four figures and indicates the current speeds computed by the model. $\mathbf{u}^*$ is the maximal speed value. The circulation forms two large counterclockwise eddies in July that split into smaller eddies in autumn. Then, some mid-scale eddies appear in January and April.

3.3 Residence time study in the Gulf of Salwa

Now, let us analyze the results of the LPT. The objective was to assess the residence time in the Gulf of Salwa. We ran a simulation over 6 months between January 6th and July 5th 2021, and used it as input of the LPT algorithm of SLIM. All parameters and details of the algorithm are detailed in section 2.2.

On figure 3.7, we see the domain D which is the region from where the particles were released. Its open boundaries are the green lines in the northern Gulf of Salwa and its closed boundaries are the coasts of Saudi Arabia to the west, those of Qatar to the east and Bahrain to the north. The figure represents the final residence times of each element in D, namely $\theta_i(t_n)$ (see equation 2.7) for all triangles i in D (t_n is thus 5/07/2021). The weighted average residence time $\bar{\theta}$, which is computed with equation 2.8, equals 127.09 days.

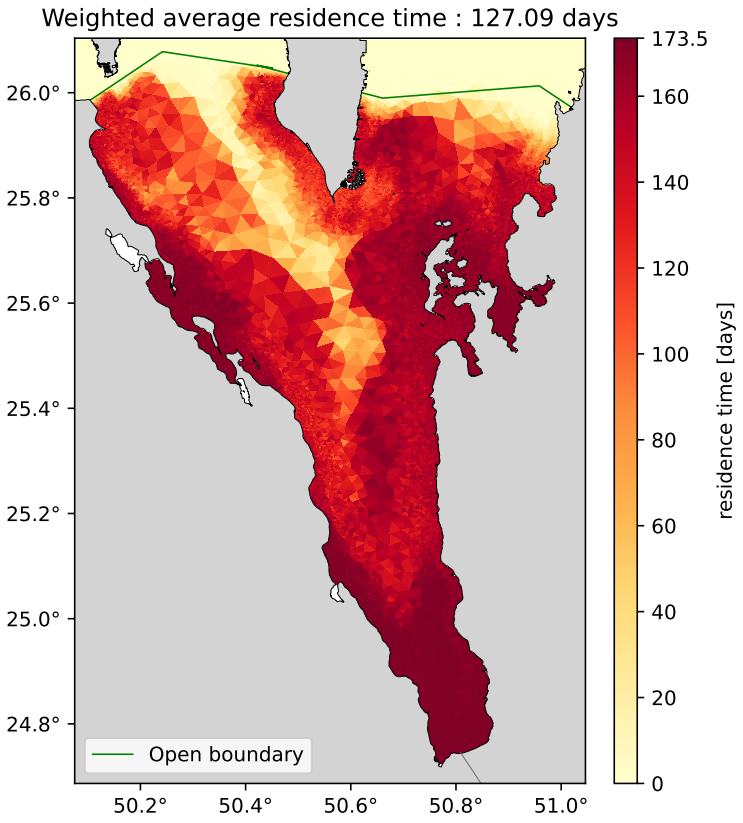

Figure 3.7: Elemental residence times $\theta_i(t_n)$ for the region of the Gulf of Salwa, called D. The open boundaries (limits of D) are the green lines. The average residence time is very long, some particles did not even leave D.

We see that a large majority of the particles take more than 100 days to leave D. Just as a reminder, particles are transported by the currents modelled by SLIM and by a random diffusivity term. We say that they leave D when their position crosses an open boundary. Moreover, particles that started in the very southern part of the GoS, or in narrow regions in the center west and east of the domain do not even manage to leave D in the allotted time. This is actually the case for 72.9% of the released particles, which is quite a lot. This means those particles take at least more than 6 months to leave the GoS, which is quite a big amount of time.

By looking at figure 3.8, we can further analyze this phenomenon. The figure represents the streamlines and current speeds, in the same way as in section 3.2, but for January and June 2021. This corresponds to the first and last month of the simulation time. We see that most current speeds in the GoS have an order of magnitude of 1 cm/s. We can reasonably assume that D is about 133 km long (see figures 1.1, 3.1) from the very south of the GoS to the middle of Bahrain. If we compute the time for a particle having 100 km to cover to flow up to the open boundary at 1 cm/s, it gives $100 \times 10^5 \times \frac{1}{3600 \times 24} \approx 116$ days. This is quite consistent with $\bar{\theta} = 127.09$ days. This shows that the LPT is consistent with the flows computed by the model and that its results are realistic.

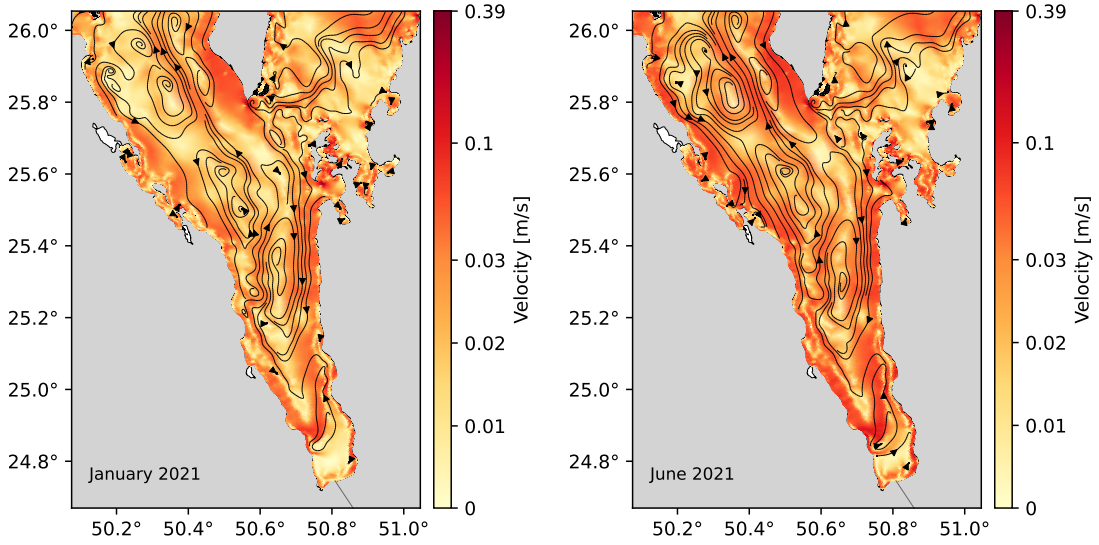

Figure 3.8: Streamplots of the Gulf of Salwa for January and June 2021. As in section 3.2, the current directions and speeds are shown. The velocities of $\mathbf{u}$ are smaller in this narrow region than in the rest of the Gulf.

Coming back to figure 3.7, we see that the sort of corridor of short residence times going from the north-west to the south-east, in the northwestern part of the GoS is also consistent with the streamlines. Indeed, in June 2021, the currents are going up the GoS in that same part. Also, the fact that the gradient of colors is not constant everywhere can be explained by two factors. First, there is a random diffusivity term, which makes the particles released from a common point to move in different directions. Secondly, there are not that many released particles (30 per triangle, for 20678 triangles), so that random factor does not get the opportunity to be fully smoothed.

Finally, we could wonder why the largest residence times on figure 3.7 are 173.5 days, whereas the simulation lasts 181 days. This is just because the particles are released during a 15 days period. In consequence, some will only be moving around in D for 166 days, while others will stay within it for 181 days. For this reason, elements for which none of the released particles has escaped from D (the darkest red triangles on the figure) will have a residence time that simplifies as $181 - \frac{15}{2} = 173.5$ days.

Chapter 4

Discussion

Let us now try to interpret the results we obtained from this work and position them in relation to other studies made on the subject.

Generally speaking, the results of the SLIM2D model are fairly consistent with other results presented in the introduction. The gyre taking place between April and July corresponds quite well to what was spotted by many (Pous, Lazure, and Carton 2015 and Thoppil and Hogan 2010). The fact that it separates in several smaller eddies in autumn was also recorded by the previous studies. However, the model set up here shows that a gyre, even if is it not as big as in summer, is already formed in winter (January). This was not the case in other studies, so the model brings also some differences.

Plus, the model also highlights the inter-annual variations in the Gulf's circulation. This confirms what have been introduced by Pous, Lazure, and Carton 2015 and Thoppil and Hogan 2010. The same thing can be said for the water masses exchanges. It happens the most during summer, because of the high evaporation rates during that period. This will create important gradients of temperature and salinity and make the water layers slide on each other. Again, these water exchanges through the Strait of Hormuz see many inter-annual changes.

The least that we can say about the Gulf's circulation is that it is rather complex. It shows inter-seasonal and inter-annual variabilities that are much influenced by stratifications, as just mentioned. Unfortunately, this cannot by fully understood by a two-dimensional model. Indeed, a three dimensional model would be able to model the water temperatures, salinities, pressions and three-dimensional velocities. Such a model would then allow to better capture the reasons of the changes in the circulation described here.

Regarding the study made on the Gulf of Salwa with the Lagrangian particle tracker, the results are also confirming what was expected. The very large mean residence time in the GoS means that it is not very connected with the rest of the Gulf. Particles are struggling to escape and this is explained by two main factors. Firstly, the current velocities there are small (< 0.1 m/s) which makes it difficult for the particles to move very far away from their initial position in a short amount of time. On the other hand, the region is pretty narrow and long and there are many little islands near the coasts, which makes communication with the rest of the Gulf especially difficult for elements located in the southern GoS. Particles released from especially narrow regions of the Gos, or behind islands will also easily be stuck at some point and will not be able to leave the domain.

Chapter 5

Conclusion

Throughout this work, we have built a two dimensional ocean circulation model for the Arabian Gulf. The objectives were to analyze the inter-seasonal to inter-annual changes in the Gulf's circulation and to study the connectivity of the Gulf of Salwa, located south of Bahrain, with the rest of the Gulf.

To achieve our goals, we have used the two-dimensional model of SLIM, which is adapted for barotropic flows and thus suited for the case of the Gulf. The model solves the depth averaged shallow water equations to compute the depth averaged velocities of the water and the sea surface elevation. After providing the model bathymetry, wind, currents and tidal forcings, we applied it on an unstructured mesh. The latter is of high resolution near the coasts (precision of 500 m) and has local element sizes of 5 km in the central parts of the Gulf.

The model was tested at Fuwairit (north of Qatar) and in Doha Bay with on-site observations. It reproduced correctly the current directions and speeds and has a 10 cm accuracy on the water elevation. Then, simulations were made for January, April, July and October 2019, 2020 and 2022. Each time, we showed the monthly averaged current velocities over the entire Gulf. The model shows an important inter-seasonal varation of the circulation : a large counterclockwise gyre is dominating the Gulf's currents in July. It splits into smaller eddies in autumn, while the velocity values decrease all around the surface of the Gulf. Then, some mid-scale eddies appear in January and April, before that the gyre attains in maximal size in summer again. We also observed some variations of this scheme between the years.

Besides of that, we used the Lagrangian particle tracker of SLIM to simulate the transport of particles released in the Gulf of Salwa. Based on a random walk formulation of the two-dimensional advection-diffusion equations, it updates the position of particles released inside the Gulf of Salwa and computes the residence

times of all elements in the region (for every triangle, it is the average time for all particles released from tha triangle to leave the GoS). The weighted average residence time is of 127 days, while some particles did not even had the time to leave the domain. The actual mean residence time is thus larger that that. This means the currents in the Gulf of Salwa have great difficulty flowing into the rest of the Gulf. We can conclude that the Gulf of Salwa is a pretty isolated part of the Arabian Gulf.

The results obtained here were pretty close to those found in previous works about the Gulf's circulation. If we wanted to push the study even further and try to get a deep understanding of all physical processes that influence the Gulf's circulation, we would need a three-dimensional model. This was originally also the goal of this work, but the model could not be ready on time. Although, I am sure such a work will be realized in the near future to complement this thesis.

Bibliography

[1] URL: https://cds.climate.copernicus.eu/#!/home (visited on 03/24/2023).

[2] Muchamad Al Azhar et al. "Modeling of Circulation in the Arabian Gulf and the Sea of Oman: Skill Assessment and Seasonal Thermohaline Structure". In: *Journal of Geophysical Research: Oceans* 121.3 (2016), pp. 1700–1720. ISSN: 2169-9291. DOI: 10.1002/2015JC011038. URL: https://onlinelibrary.wiley.com/doi/abs/10.1002/2015JC011038 (visited on 12/15/2022).

[3] Maryam R. Al Shehhi, Imen Gherboudj, and Hosni Ghedira. "An Overview of Historical Harmful Algae Blooms Outbreaks in the Arabian Seas". In: *Marine Pollution Bulletin* 86.1 (Sept. 15, 2014), pp. 314–324. ISSN: 0025-326X. DOI: 10.1016/j.marpolbul.2014.06.048. URL: https://www.sciencedirect.com/science/article/pii/S0025326X14004287 (visited on 05/22/2023).

[4] Aya Batrawy. *Oil Shippers Continue Sailing Through Strait of Hormuz - with Heightened Security*. Insurance Journal. June 21, 2019. URL: https://www.insurancejournal.com/news/international/2019/06/21/530110.htm (visited on 12/15/2022).

[5] *Coastlines*. URL: https://osmdata.openstreetmap.de/data/coastlines.html (visited on 03/23/2023).

[6] *Copernicus Marine Data Store*. URL: https://data.marine.copernicus.eu/products (visited on 03/23/2023).

[7] Eric Deleersnijder. "Numerical approximation of the residence time in a coastal lagoon". In: UCL - Université Catholique de Louvain (2017). URL: https://dial.uclouvain.be/pr/boreal/object/boreal:186065 (visited on 05/31/2023).

[8] *Discontinuous Galerkin Method*. In: *Wikipedia*. Mar. 13, 2023. URL: https://en.wikipedia.org/w/index.php?title=Discontinuous_Galerkin_method&oldid=1144342423 (visited on 03/21/2023).

[9] Thomas Dobbelaere. "Numerical Study of Whitings Formation on the Bahama Bank". 2018.

[10] *Fossil Fuel Consumption*. Our World in Data. URL: https://ourworldindata.org/grapher/fossil-fuel-primary-energy (visited on 12/14/2022).

[11] Christophe Geuzaine and Jean-François Remacle. "Gmsh: A 3-D Finite Element Mesh Generator with Built-in Pre- and Post-Processing Facilities". In: *International Journal for Numerical Methods in Engineering* 79.11 (2009), pp. 1309–1331. ISSN: 1097-0207. DOI: 10.1002/nme.2579. URL: https://onlinelibrary.wiley.com/doi/abs/10.1002/nme.2579 (visited on 03/22/2023).

[12] Olivier Gourgue. "Finite Element Modeling of Sediment Dynamics in the Scheldt". In: ().

[13] *Gulf War Oil Spill*. In: *Wikipedia*. Apr. 13, 2023. URL: https://en.wikipedia.org/w/index.php?title=Gulf_War_oil_spill&oldid=1149692247#Background (visited on 05/13/2023).

[14] Emmanuel Hanert et al. "A Multiscale Ocean Modelling System for the Central Arabian/Persian Gulf: From Regional to Structure Scale Circulation Patterns". In: *Estuarine, Coastal and Shelf Science* 282 (Mar. 5, 2023), p. 108230. ISSN: 0272-7714. DOI: 10.1016/j.ecss.2023.108230. URL: https://www.sciencedirect.com/science/article/pii/S0272771423000203 (visited on 03/31/2023).

[15] Hans Hersbach et al. "The ERA5 Global Reanalysis". In: *Quarterly Journal of the Royal Meteorological Society* 146.730 (2020), pp. 1999–2049. ISSN: 1477-870X. DOI: 10.1002/qj.3803. URL: https://onlinelibrary.wiley.com/doi/abs/10.1002/qj.3803 (visited on 03/24/2023).

[16] F. Hosseinibalam, S. Hassanzadeh, and A. Rezaei-Latifi. "Three-Dimensional Numerical Modeling of Thermohaline and Wind-Driven Circulations in the Persian Gulf". In: *Applied Mathematical Modelling* 35.12 (Dec. 1, 2011), pp. 5884–5902. ISSN: 0307-904X. DOI: 10.1016/j.apm.2011.05.040. URL: https://www.sciencedirect.com/science/article/pii/S0307904X11003519 (visited on 05/25/2023).

[17] J. R. Hunter, P. D. Craig, and H. E. Phillips. "On the Use of Random Walk Models with Spatially Variable Diffusivity". In: *Journal of Computational Physics* 106.2 (June 1, 1993), pp. 366–376. ISSN: 0021-9991. DOI: 10.1016/S0021-9991(83)71114-9. URL: https://www.sciencedirect.com/science/article/pii/S0021999183711149 (visited on 05/30/2023).

[18] *Introducing ChatGPT*. URL: https://openai.com/blog/chatgpt (visited on 06/05/2023).

[19] T. V. Joydas et al. “Status of Macrobenthic Communities in the Hypersaline Waters of the Gulf of Salwa, Arabian Gulf”. In: *Journal of Sea Research* 99 (May 1, 2015), pp. 34–46. ISSN: 1385-1101. DOI: 10.1016/j.seares.2015.01.006. URL: https://www.sciencedirect.com/science/article/pii/S1385110115000143 (visited on 05/25/2023).

[20] *Managing Water for Peace in the Middle East*. URL: https://archive.unu.edu/unupress/unupbooks/80858e/80858E09.htm (visited on 05/22/2023).

[21] General Bathymetric Chart of the Oceans. *Gridded Bathymetry Data (General Bathymetric Chart of the Oceans)*. GEBCO. URL: https://www.gebco.net/data_and_products/gridded_bathymetry_data/ (visited on 03/22/2023).

[22] *Oil Development in the Middle East*. Institution of Civil Engineers (ICE). URL: https://www.ice.org.uk/what-is-civil-engineering/what-do-civil-engineers-do/oil-development-in-the-middle-east/ (visited on 12/14/2022).

[23] Akira Okubo. “Oceanic Diffusion Diagrams”. In: *Deep Sea Research and Oceanographic Abstracts* 18.8 (Aug. 1, 1971), pp. 789–802. ISSN: 0011-7471. DOI: 10.1016/0011-7471(71)90046-5. URL: https://www.sciencedirect.com/science/article/pii/0011747171900465 (visited on 05/31/2023).

[24] *OSU TPXO Tide Models - TPXO9-atlas*. URL: https://www.tpxo.net/global/tpxo9-atlas (visited on 03/24/2023).

[25] *Persian Gulf History,Arabian Gulf, Pars Sea ,* URL: http://www.persiangulfstudies.com/en/index.asp?p=pages&id=213 (visited on 12/14/2022).

[26] *Plans*. Apple (France). URL: https://www.apple.com/fr/maps/ (visited on 03/30/2023).

[27] Stéphane Pous, Pascal Lazure, and Xavier Carton. “A Model of the General Circulation in the Persian Gulf and in the Strait of Hormuz: Intraseasonal to Interannual Variability”. In: *Continental Shelf Research* 94 (Feb. 15, 2015), pp. 55–70. ISSN: 0278-4343. DOI: 10.1016/j.csr.2014.12.008. URL: https://www.sciencedirect.com/science/article/pii/S027843431400363X (visited on 12/15/2022).

[28] *QGIS*. URL: https://www.qgis.org/fr/site/ (visited on 03/22/2023).

[29] “Seasonal Cycles of Temperature, Salinity and Water Masses of the Western Arabian Gulf”. In: ().

[30] *SLIM – Second-generation Louvain-la-Neuve Ice-ocean Model*. URL: https://www.slim-ocean.be/ (visited on 12/16/2022).

[31] J. Smagorinsky. “GENERAL CIRCULATION EXPERIMENTS WITH THE PRIMITIVE EQUATIONS: I. THE BASIC EXPERIMENT”. In: *Monthly Weather Review* 91.3 (Mar. 1, 1963), pp. 99–164. ISSN: 1520-0493, 0027-0644. DOI: 10.1175/1520-0493(1963)091<0099:GCEWTP>2.3.CO;2. URL: https://journals.ametsoc.org/view/journals/mwre/91/3/1520-0493_1963_091_0099_gcewtp_2_3_co_2.xml (visited on 03/22/2023).

[32] S. D. Smith and E. G. Banke. “Variation of the Sea Surface Drag Coefficient with Wind Speed”. In: *Quarterly Journal of the Royal Meteorological Society* 101.429 (1975), pp. 665–673. ISSN: 1477-870X. DOI: 10.1002/qj.49710142920. URL: https://onlinelibrary.wiley.com/doi/abs/10.1002/qj.49710142920 (visited on 03/22/2023).

[33] Aurélien Soupart. “Modelling Marine Connectivity in the Great Barrier Reef”. 2018.

[34] S. Spagnol et al. “An Error Frequently Made in the Evaluation of Advective Transport in Two-Dimensional Lagrangian Models of Advection-Diffusion in Coral Reef Waters”. In: *Marine Ecology Progress Series* 235 (June 19, 2002), pp. 299–302. ISSN: 0171-8630, 1616-1599. DOI: 10.3354/meps235299. URL: https://www.int-res.com/abstracts/meps/v235/p299-302/ (visited on 05/30/2023).

[35] Prasad G. Thoppil and Patrick J. Hogan. “A Modeling Study of Circulation and Eddies in the Persian Gulf”. In: *Journal of Physical Oceanography* 40.9 (Sept. 1, 2010), pp. 2122–2134. ISSN: 0022-3670, 1520-0485. DOI: 10.1175/2010JPO4227.1. URL: https://journals.ametsoc.org/view/journals/phoc/40/9/2010jpo4227.1.xml (visited on 12/16/2022).

[36] Louis Verbiest. “Investigating the Dispersal of Hawksbill Sea Turtle Hatchlings in the Arabian Gulf”. 2022.

UNIVERSITÉ CATHOLIQUE DE LOUVAIN
École polytechnique de Louvain
Rue Archimède, 1 bte L6.11.01, 1348 Louvain-la-Neuve, Belgique | **www.uclouvain.be/epl**